Energy and Buildings 85 (2014) 549–559

Contents lists available at ScienceDirect

Energy and Buildings

journal homepage: www.elsevier.com/locate/enbuild

Modeling environment for model predictive control of buildings

T. Zakula [a,*], P.R. Armstrong [b], L. Norford [c]

[a] University of Zagreb, FAMENA, I. Lucica 5, 10000 Zagreb, Croatia
[b] Masdar Institute of Science and Technology, Masdar City, Abu Dhabi, United Arab Emirates
[c] Massachusetts Institute of Technology, 77 Massachusetts Avenue, Cambridge, 02139 MA, USA

ARTICLE INFO

Article history:
Received 7 April 2014
Received in revised form
21 September 2014
Accepted 23 September 2014
Available online 2 October 2014

Keywords:
Model predictive control
Simulation tool
Energy efficiency

ABSTRACT

Model predictive control (MPC) is an advanced control that can be used for dynamic optimization of HVAC equipment. Although the benefits of this technology have been shown in numerous research papers, currently there is no commercially or publicly available software that allows the analysis of building systems that employ MPC. The lack of detailed and robust tools is preventing more accurate analysis of this technology and the identification of factors that influence its energy saving potential. The modeling environment (ME) presented here is a simulation tool for buildings that employ MPC. It enables a systematic study of primary factors influencing dynamic controls and the savings potential for a given building. The ME is highly modular to enable easy future expansion, and sufficiently fast and robust for implementation in a real building. It uses two commercially available computer programs, with no need for source code modifications or complex connections between programs. A simplified building model is used during the optimization, whereas a more complex building model is used after the optimization. It is shown that a simplified building model can adequately replace a more complex model, resulting in significantly shorter computational times for optimization than those found in the literature.

1. Introduction

Model predictive control (MPC) is an optimal control that uses a dynamic system model and predictions of future events to optimize the objective function (e.g. energy consumption or cost). MPC is already used in some process industries, and is becoming an increasingly popular research topic in buildings, demonstrating the benefits for building energy consumption and electricity cost. Based on weather and load predictions, MPC enables energy efficient strategies through the optimization of heating, ventilation and air conditioning (HVAC) system operation, while ensuring thermal comfort for occupants. For example, it can predict optimal shifting of cooling loads to night time, when the outside temperatures are lower and, therefore, the efficiency of cooling equipment is higher. Furthermore, it can result in lower cooling cost in case of utility rates that favor night operation, as well as reduction in peak loads.

The benefits of MPC for building HVAC systems have been demonstrated in numerous papers found in the literature, mainly using numerical simulations. The previous research showed that the use of MPC can result in 5–70% energy savings and 10–45% peak power savings [1–9]. The reported savings were demonstrated for both heating and cooling systems, and were strongly dependent on a climate, building type, system type and simulation assumptions. One of the crucial elements for MPC is a building model suitable for capturing a building's dynamic behavior since it can strongly influence the optimization accuracy and computational speed. Recently, important work was done on various building models for the MPC application [10–16]. Based on a comparison of models ranging from those that make use of a system's physical description to black-box models, Prívara et al. [17] suggested that methods using a physical description should be used primarily for buildings with simpler structures, while black-box models (e.g. subspace identification [18]) are much more suitable for complex structures. Prívara et al. [15] also showed that a model with a reduced set of inputs and states can have similar accuracy as a model with a full set. A weather forecast is another element that strongly influences the prediction accuracy of MPC. In a comparison of short-term weather forecasting models, Krarti and Henze [3] suggested that the bin model (which uses observations from the previous 30 and 60 days) had the best prediction accuracy. The use of this model resulted in marginally different cost savings compared to the case with perfect weather knowledge. Using the modeling environment developed by Krarti et al. [19], Henze et al. [20] also investigated different lengths of the planning horizon, where the planning horizon represents the time interval over which the cost function was evaluated.

* Corresponding author. Tel.: +385 981820552.
E-mail address: tzakula@fsb.hr (T. Zakula).

http://dx.doi.org/10.1016/j.enbuild.2014.09.039
0378-7788/

Nomenclature

COP	coefficient of performance (–)
c	specific heat (J/(kg K))
L	latent load (kg_w/s)
m	mass flow rate (kg/s)
OF	objective function (–)
P	power (W)
p	pressure (Pa)
Q	heating or cooling rate (W)
T	temperature (°C)
V	volume flow rate (m^3/s)
w	absolute humidity (kg_w/kg_{air})
ρ	density (kg/m^3)

Subscripts

adj	adjacent room
air	air
as	assumed
avg	average
c	condensing
cc	cooling coil
conv	convective
e	evaporating
hp	heat pump
i	internal
in	inlet
llim	lower limit
m	measured
max	maximal
o	operative
opt	optimal
rad	radiative
return	return (water)
s	supply (air)
supply	supply (water)
trans	transport
ulim	upper limit
w	water
x	ambient
z	zone

Results showed that the planning horizon on the order of 24 h is only marginally sub-optimal compared to the horizon over a simulation period of one week. Moroşan et al. [21] tested different MPC strategies for multi-zone buildings by comparing decentralized MPC, in which each zone temperature is regulated by its own controller, with centralized MPC, in which the entire multi-zone system is controlled by one MPC law. Due to the lack of thermal coupling with decentralized MPC and high computational demand with centralized MPC, the authors proposed distributed MPC with local MPCs for each zone and a communication network between them. This approach allowed for coupling between the subsystems, and resulted in reduced computational demand relative to the centralized approach.

Only a few papers have given detailed descriptions of the tools used to simulate a building with MPC. Krarti and Henze [3] provided an in-depth overview of a simulation model in which EnergyPlus was modified and integrated with the optimization software GenOpt. The additional model was done in TRNSYS, using a version of the TRNSYS source code not commercially available [22]. Optimizing a day with 24 hourly setpoints took 1–4 h for the Nelder–Mead simplex method and 8–29 h with the OptQuest (population-based scatter search) method. Spindler and Norford [23] and May-Ostendorp et al. [24] showed that MPC can also be successful in optimizing a mixed-mode building behavior. While Spindler and Norford [23] used the data-driven, inverse model trained on a real building, May-Ostendorp et al. [24] employed the combination of EnergyPlus and MATLAB environments. Using the particle swarm optimization, May-Ostendorp et al. [24] optimized window operation in a mixed model building with a 24-h planning horizon and a 2-h optimization block. This resulted in 12 optimization variables of binary window decisions (window in position 0 or 1). The reported simulation time for 11 weeks in summer was 12 h. Corbin et al. [25] described a framework for MPC that combines EnergyPlus and MATLAB and uses the particle swarm optimization. The algorithm can be used for MPC of different building systems, which was shown for a VAV system and for a building with TABS. In the first example, having 14 daily temperature setpoints as optimization variables resulted in the simulation time of 26 clock hours to simulate one week. In the second example, it took one day of clock time to simulate one day for a building with 11 thermal zones and 12 optimization variables. Coffey et al. [26] developed a software framework for MPC that combines GenOpt and SimCon with any building energy simulation program that can read and write into a text file. The connection between SimCon and the energy modeling software TRNSYS was enabled through the building control virtual test bed [27]. To optimize one day using MPC, the reported computational time was three nights.

Although the benefits of MPC have been demonstrated in numerous research papers, important challenges that still remain are the lack of tools for the system analysis and practical challenges facing real building implementation. Findings in the literature on potential energy and cost savings are highly dependent on a variety of factors, such as the building type, internal load, climate, equipment characteristics, and controls. The use of a computer model allows for a systematic study of primary factors influencing the dynamic control and savings potential for an individual building. However, currently there are no commercially or public available tools for this type of analysis. Of the few papers in the literature that give detailed descriptions of the tools used to simulate building with MPC, most require modification of existing building simulation programs, which has been shown as challenging. One example is a severe issue with initialization of variables in building software EnergyPlus and TRNSYS, as mentioned in more detail later in this paper. Furthermore, the reported computation times are not practical for implementation in real buildings where the optimization usually needs to be repeated each hour due to uncertainties in load and weather predictions. The implementation in real buildings is somewhat inhibited by control complexity compared to conventional systems. Examples are found in the literature of simplified control strategies that would result in a near-optimal control [28], but those strategies are still obtained by using more detailed computer models.

The modeling environment (ME) presented here simulates the performance of a building in which HVAC systems are operated using MPC. It can be set to optimize a variety of HVAC systems and optimization objectives, using different planning horizons (the time interval over which the objective function is evaluated) and execution horizons (the time interval over which the control strategy is applied). The ME does not require any modification of existing building programs, only the common connection between Matlab and TRNSYS (using TRNSYS Type 155). To reduce computational time, the ME uses two building models of different complexities, where the simplified model is used in the optimization, and TRNSYS only for post optimization. This avoids complex connections between different programs and results in significantly shorter computational time, making the ME robust and suitable for implementation in real buildings.

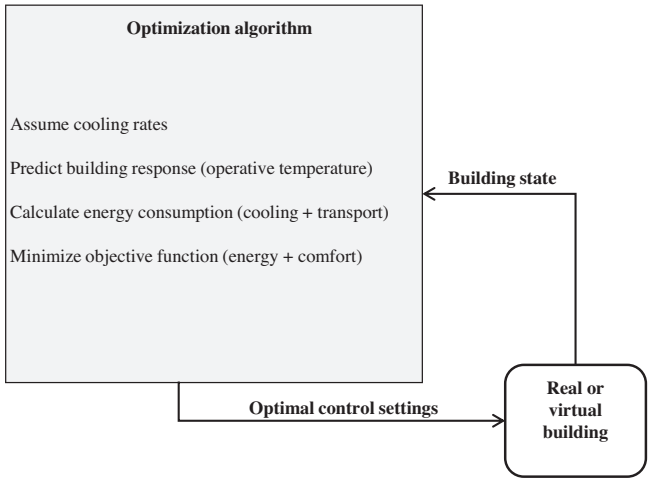

Fig. 1. Scheme of modeling environment for MPC simulation.

2. Model description

Here we describe the modeling environment (ME) for the example of a cooling system controlled to minimize electricity consumption. The example will include cooling with thermally activated building surfaces (TABS) and a variable-air-volume (VAV) system. Different objectives, such as the total cost of electricity/fuel for cooling/heating, can be achieved by modifying the objective function.

The basic scheme of minimizing a building's electricity consumption is shown in Fig. 1. With the planning horizon of 24 h, the optimization algorithm is executed day-by-day, making a first guess of cooling rates in each hour (24-variable optimization). The optimization variable for the VAV system is a sensible cooling rate imposed on the room, whereas the optimization variable for cooling with TABS is a chiller cooling rate, different than the instantaneous cooling rate imposed on the room due to the TABS thermal lag. The objective function that needs to be minimized is a sum of the total daily electricity for cooling, electricity for transport and the temperature penalty. Introducing the temperature penalty is an implicit way of ensuring thermal comfort for the occupants.

To determine whether the proposed strategy leads to comfortable building conditions, the ME incorporates a building model capable of predicting transient thermal response of the occupied zones. Thermal comfort is influenced by both air and surface temperatures, which becomes especially relevant for cooling/heating with TABS. Compared to all-air systems, the benefit of cooling with TABS is that people feel equally comfortable at slightly higher air temperatures due to large, cold surfaces. To account for the combined effect of air and surface temperatures, the operative temperature, rather than the air temperature, was chosen as the controlled temperature. In a real building, where surface temperature measurements are usually not available, a more practical solution would be to use the room air temperature as the control variable, but setting the temperature setpoint 1–2 °C higher when cooling with TABS than when cooling with the VAV system.

After optimization using the simplified building model, the optimal control settings are passed to either a real or a virtual building. Parameters that will be passed depend on the type of cooling system; for example, the parameter used as the input for the building with the VAV system is the volumetric flow rate of air (assuming constant supply temperature), and the input for the building with TABS is the water supply temperature (assuming constant mass flow rate).

2.1. Building model

When predicting a control strategy that minimizes the cost function (e.g. the price of electricity or the total electricity consumption) it is necessary to capture a building's thermal and hygric response. The thermal response is used to ensure thermal comfort for the occupants, while the hygric response becomes especially relevant for cases in which a room's humidity needs to be tightly controlled. For example, if the humidity of a room cooled with thermally activated building surfaces (TABS) is not controlled, condensation can occur due to cold surfaces. The intention here was to develop a MPC analysis tool that can be widely used, and be fast enough for implementation in a real building. Due to uncertainty in weather and internal gain predictions, the optimization in real buildings usually needs to be repeated more frequently (e.g. each hour), putting a relatively strict constraint on the computational time. This influenced the selection of a building model; only commercially available tools that give a fast building response were considered.

Many commercially available building energy simulation programs (BESP) offer more or less detailed simulation of a building's dynamic behavior. There are numerous programs for whole building energy simulations such as DOE-2, DesignAdvisor, eQUEST, CAMSOL, SPARK, TARP and Modelica. A complete list and overview of program capabilities can be found in the Building Energy Software Tools Directory [43]. Most of BESPs are focused on thermal calculations, while analyzing moisture transfer with simplified methods that do not account for a change of material properties with variations in temperature and humidity, nor do they account for a change in the moisture buffer effect due to a temperature gradient in a wall. The simplified method often used to describe moisture transfer between the air and solids is the effective moisture penetration depth (EMPD) theory proposed by Kerestecioglu et al. [29]. Due to a lack of programs that combine airflow, heat transfer and moisture transfer processes in buildings, Annex 41 of the International Energy Agency (IEA) had the goal of stimulating the development of information and analytical tools. Rode and Woloszyn [30] gave a detailed overview of the IEA project, description of common exercises, advances in simulation programs and papers published on the topic.

Two widely used programs developed to capture a building's transient behavior are EnergyPlus [31] and TRNSYS (Transient System Simulation Program, Klein et al. [32]). These programs are often used in academic research since they enable a detailed analysis of complex building systems. Numerous research papers can be found on their use for variety of building analyses, with TRNSYS more often used in Europe and EnergyPlus in the U.S. TRNSYS has been chosen for the MPC modeling environment as a comprehensive and modular simulation tool that is somewhat more suitable for building control system analysis. EnergyPlus was not originally designed for a detailed analysis of building control systems, but can be linked to programs more suitable for system controls, such as MATLAB or Simulink. The connection can be done through building controls virtual test bed (BCVTB) developed by Lawrence Berkeley National Laboratory. However, both TRNSYS and EnergyPlus proved to be challenging for the MPC application due to their inability to explicitly initialize all variables at the beginning of a new planning horizon period. For example, a user can explicitly define the initial room air temperature before a simulation starts, and that temperature is also assumed to be the initial wall temperature. Since the thermal mass temperature can be significantly different than the room temperature in the building with TABS, the inability to explicitly define different wall initial conditions represents a severe issue.

Both the issue of computational speed and especially the issue of initialization of variables were motives to consider the use of an alternative model for the optimization algorithm. The chosen

alternative model is the inverse model based on a comprehensive room transfer function developed by Seem [33]. Seem [33] showed that the transfer functions used to describe transient changes for individual surfaces can also be used to describe transient changes of a whole room. In the derived comprehensive room transfer function (CRTF), a heat flux for a room was calculated as a weighted sum of past heat rates and instantaneous and past temperatures. The number of past terms depends on the "heaviness" of the mass, where more past terms are relevant for a heavier construction. Armstrong et al. [34] showed that the CRTF coefficients for heat flux response are generally not best for temperature response (iCRTF). In their proposed model, a temperature is a weighted sum of past zone temperatures and current and past ambient temperatures and heat rates:

$$T_z = \sum_{t=1}^{n} a^t T_z^t + \sum_{t=0}^{n} b^t T_x^t + \sum_{t=0}^{n} c^t q^t \quad (1)$$

where the coefficients a, b and c must satisfy the Fourier's law of conduction in steady state and therefore, the constraint for the inverse model coefficients is:

$$1 - \sum_{t=0}^{n} a^t = \sum_{t=0}^{n} b^t \quad (2)$$

Gayeski [35] showed that the inverse model can serve for a fast and reliable implementation of MPC in a real building. He used the linear regression on a few weeks of training data to find the model coefficients, and then used the inverse model to predict room temperatures in the 24-h-ahead TABS cooling optimization. Gayeski also analyzed the dependence of prediction accuracy on number of past terms for a specific case. He showed that a higher number of terms does not necessarily give better predictions due to the strong effect of system noise on parameters of high-order identified models.

While the simplified, inverse building model is used for the optimization, a more detailed building model in TRNSYS is used to find inverse model coefficients and validate the inverse model. Moreover, it is employed as a virtual building to give a more accurate building response on optimal control after the optimization.

2.1.1. TRNSYS model

A room cooled with the VAV system and parallel TABS (cooling through floor slab) has been modeled in TRNSYS. The modeled room is the experimental room located at Massachusetts Institute of Technology (MIT), USA, and it was chosen since experimental measurements for a typical summer week in Atlanta [35] could be used to validate the accuracy of the TRNSYS model. The room is divided into the climate room and test room, both adjacent to the larger laboratory room. The walls are made of two 16 mm gypsum layers, with 110 mm of a polyisocyanurate foam placed in between. There are three double-pane windows between the test room and the climate room. The test room floor has PEX pipes embedded into the commercially available subfloor system and is covered with three layers of concrete pavers. Details on the room construction are given in the Appendix. The pipes can be used for hydronic sensible cooling or heating. The room has an additional indoor unit (VRF system) for direct heating, cooling and dehumidification. Both systems are served by the common outdoor unit, which is placed in the climate room so that it captures changes in the chiller efficiency with respect to ambient conditions. The test room is also equipped with lights and heat sources that can simulate internal convective and radiative heat gains for a typical office building. The test room was not exposed to solar gains nor wind. The climate room temperature is controlled by a separate air heating and cooling system, allowing for testing different climate conditions. The experimental measurements were not performed for the hygric response of the MIT's experimental room. Therefore, parameters used in the TRNSYS buffer storage model for hygric response are those given in the TRNSYS example for a typical office. The office is approximately of the same volume as MIT's experimental room, with walls made of 12 mm gypsum and 100 mm mineral wool and the floor and ceiling made of concrete.

Table 1
Relative RMS prediction errors for comparison between TRNSYS model and experimental measurements.

Relative RMSE			
T_z	$T_{w,return}$	T_{floor}	Q_{TABS}
0.0512	0.0040	0.0339	0.0256

Experimental measurements that were inputs to the TRNSYS model for model validation are the climate room temperature, laboratory room temperature, floor temperature below TABS, internal loads, supply water temperature, and water mass flow rate. Cases were run in TRNSYS with time steps of 1, 15, and 30 min to ensure that the results are not affected by our choice of time step. The relative RMS error for predicted air temperature response, return water temperature, floor temperature and TABS cooling rate (Table 1) show good agreement with the measured data. The prediction errors were calculated as:

$$\text{RelativeRMSE} = \text{mean}\sqrt{\left(\frac{X_{\text{measurements}} - X_{\text{TRNSYS}}}{\max(X_{\text{measurements}}) - \min(X_{\text{measurements}})}\right)^2} \quad (3)$$

2.1.2. Inverse model for thermal response

Here we show how Eq. (1) can be modified to describe the thermal response of a single zone cooled by the VAV system and parallel TABS. The equation is used to calculate the air temperature T_z, operative temperature T_o, floor temperature T_{floor} and water return temperature (from TABS) $T_{w,return}$. The VAV system sensible cooling represents an instantaneous convective cooling rate, whereas the internal loads have a certain convective-to-radiative heat transfer split. Therefore, to improve the inverse model predictions in cases when the VAV system and internal loads are acting together, the third term in Eq. (1) is split into a convective and radiative term. Cooling with the TABS is also treated as a separate term, since it is accounted for in the instantaneous chiller cooling rate, different than the instantaneous zone's cooling rate due to the thermal lag.

Modified equations are:

$$T_z = \sum_{t=1}^{n} a_z^t T_z^t + \sum_{t=0}^{n} b_z^t T_{adj}^t + \sum_{t=0}^{n} c_z^t T_x^t + \sum_{t=0}^{n} d_z^t Q_{TABS}^t + \sum_{t=0}^{n} e_z^t Q_{conv}^t + \sum_{t=0}^{n} f_z^t Q_{rad}^t \quad (4)$$

$$T_o = \sum_{t=1}^{n} a_o^t T_o^t + \sum_{t=0}^{n} b_o^t T_{adj}^t + \sum_{t=0}^{n} c_o^t T_x^t + \sum_{t=0}^{n} d_o^t Q_{TABS}^t + \sum_{t=0}^{n} e_o^t Q_{conv}^t + \sum_{t=0}^{n} f_o^t Q_{rad}^t \quad (5)$$

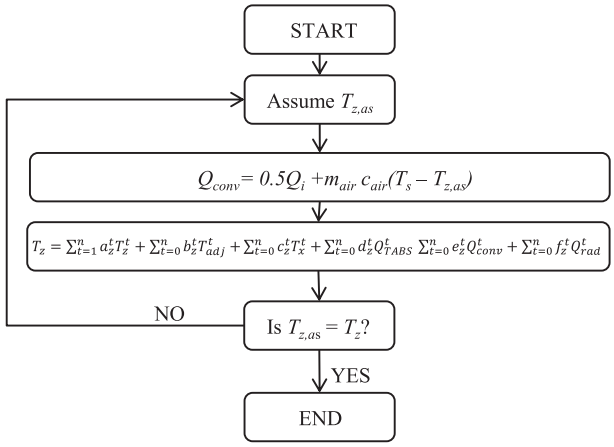

Fig. 2. Iteration loop for VAV system cooling rates.

$$T_{\text{floor}} = \sum_{t=1}^{n} a_{\text{f}}^t T_{\text{floor}}^t + \sum_{t=0}^{n} b_{\text{f}}^t T_{\text{adj}}^t + \sum_{t=0}^{n} c_{\text{f}}^t T_{\text{x}}^t + \sum_{t=0}^{n} d_{\text{f}}^t Q_{\text{TABS}}^t + \sum_{t=0}^{n} e_{\text{f}}^t Q_{\text{conv}}^t + \sum_{t=0}^{n} f_{\text{f}}^t Q_{\text{rad}}^t \quad (6)$$

$$T_{\text{w,return}} = \sum_{t=1}^{n} a_{\text{w}}^t T_{\text{w,return}}^t + \sum_{t=0}^{n} b_{\text{w}}^t T_{\text{floor}}^t + \sum_{t=0}^{n} c_{\text{w}}^t Q_{\text{TABS}}^t \quad (7)$$

where Q_{rad} accounts for 50% of the internal loads from people, equipment and lights, and Q_{conv} for the other 50% of the internal loads and 100% of the additional cooling/heating. T_{adj} is the temperature of adjacent rooms. The cooling rate of the chiller is calculated as:

$$Q_{\text{TABS}} = m_{\text{w}} c_{\text{w}} (T_{\text{w,return}} - T_{\text{w,supply}}) \quad (8)$$

The coefficients (a, b, c, d, e, f) can be found from the linear regression on training data created by the TRNSYS model, or from real building measurements.

If the room has only TABS cooling, without the parallel VAV system, Eqs. (4)–(6) can be simplified by combining internal loads into one term, and calculating the zone temperature, operative temperature and floor temperature as:

$$T = \sum_{t=1}^{n} a^t T^t + \sum_{t=0}^{n} b_{\text{z}}^t T_{\text{adj}}^t + \sum_{t=0}^{n} c_{\text{z}}^t T_{\text{x}}^t + \sum_{t=0}^{n} d_{\text{z}}^t Q_{\text{TABS}}^t + \sum_{t=0}^{n} e_{\text{z}}^t Q_{\text{i}}{}^t \quad (9)$$

To calculate the zone temperatures using Eqs. (4)–(6), the cooling rates delivered to the room by the VAV system must be known. However, the variables that are known in real buildings are the supply airflow rate and supply temperature, while the amount of delivered cooling depends on the zone temperature. To solve this coupling between the air temperature and cooling rates, the iteration loop shown in Fig. 2 has been added to the inverse model. Although this addition somewhat increases the computational time, the inverse model is still significantly faster than the TRNSYS model. For example, to predict the zone's thermal response for one week, it took about 0.005 seconds of real time for the inverse model without the additional interpolation loop, 0.5 s with the additional interpolation loop and 2–3 s for the TRNSYS model, all on an i7-2600 @ 3.4 GHz processor.

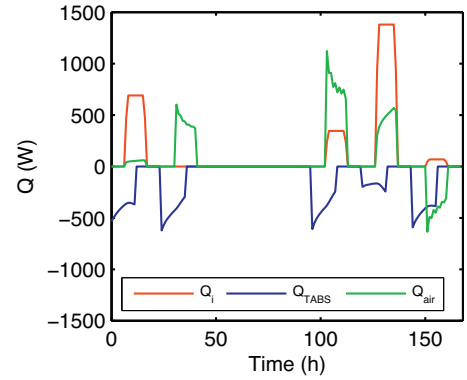

Fig. 3. TABS cooling rate (blue), VAV system cooling/heating rate (green) and internal load (red) profiles for the training data set. (For interpretation of the references to color in this figure legend, the reader is referred to the web version of this article.)

Table 2
Relative RMS prediction errors for comparison between TRNSYS and inverse model (original and modified) on two validation data sets.

	Relative RMSE			
	T_z	T_o	T_{floor}	$T_{w,return}$
Validation set 1, original	0.0008	0.0006	0.0029	
Validation set 2, original	0.0011	0.0011	0.0049	0.015
Validation set 1, modified	0.0169	0.0089	0.0026	
Validation set 2, modified	0.0322	0.0165	0.0062	0.015

Table 3
Sensitivity analysis for number of past terms in inverse model.

Number of past terms	**Relative RMSE**			
	T_z	T_o	T_{floor}	$T_{w,return}$
2	0.0308	0.0285	0.0105	0.0161
3	0.0011	0.0011	0.0049	0.0150
4	0.0012	0.0012	0.001	0.0169
6	0.0024	0.0040	0.0003	0.0278
8	0.0007	0.0015	0.0003	0.0388

2.1.3. *Validation of inverse model for thermal response*

The TRNSYS model was used to find the coefficients (a, b, c, d, e, f) from the linear regression on training data (Fig. 3) and to create two additional data sets for inverse model validation. The first validation set (Fig. 4a) represents the case with VAV system cooling, while in the second validation set (Fig. 4b) both the VAV system cooling and TABS cooling act in parallel. Three past terms were used in Eqs. (4)–(6) to account for the building's thermal lag.

The comparison between the TRNSYS and inverse model showed good agreement (Table 2) between the two models, with significantly shorter computational time for the inverse model, as reported earlier. The prediction errors in Table 2 were calculated according to Eq. (10):

$$\text{RelativeRMSE} = \text{mean}\sqrt{\left(\frac{X_{\text{TRNSYS}} - X_{\text{inverse}}}{\max(X_{\text{TRNSYS}}) - \min(X_{\text{TRNSYS}})}\right)^2} \quad (10)$$

The importance of separating purely convective cooling rates from the internal loads (that have radiative and convective component) was tested by modifying Eqs. (4)–(6). When VAV system cooling rates and internal loads were combined into one term, the results showed relatively large prediction errors for both validation sets, as shown in Table 2. The return water temperature predictions were not strongly influenced by the modifications, since the zone loads are not a direct input for the water return temperature calculation (Eq. (7)).

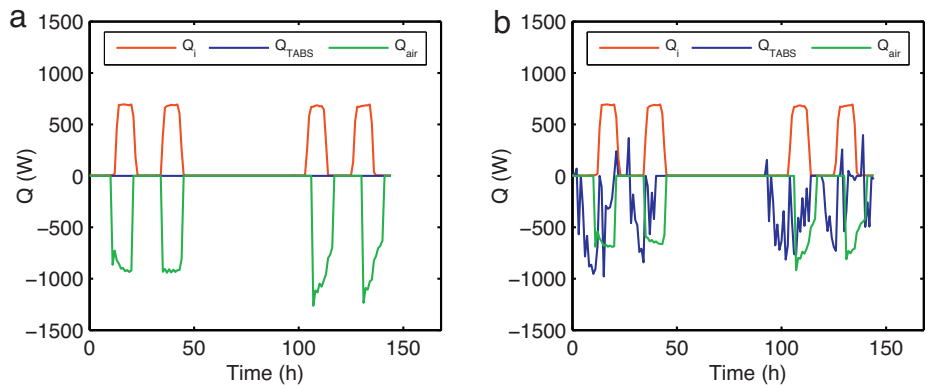

Fig. 4. TABS cooling rate (blue), VAV system cooling rate (green) and internal load (red) profiles for (a) validation set 1 and (b) validation set 2. (For interpretation of the references to color in this figure legend, the reader is referred to the web version of this article.)

The sensitivity analysis was performed on the second validation set (Fig. 4b), demonstrating the influence that the number of past terms has on the prediction accuracy. The results showed that using three past terms offers a good balance between accuracy and computational speed for this particular room (Table 3).

2.1.4. Inverse model for humidity response

When humidity in the room needs to be controlled, the modeling environment uses the inverse model for humidity response. The model is also based on a transfer function, with the zone's humidity predicted as a function of the past humidity and past and current latent loads:

$$w_z = \sum_{t=1}^{n} g^t w_z^t + \sum_{t=0}^{n} h^t L_{\text{gain}}^t \tag{11}$$

Coefficients g and h are found by a linear regression to TRNSYS data.

Similarly as for VAV system cooling rates, the latent load depends on the zone's humidity and vice versa. Therefore, the iteration loop similar to the one shown in Fig. 2 has been added to the hygric inverse model.

2.1.5. Validation of inverse model for humidity response

To validate the inverse model for humidity response, first, the coefficients g and h were found by the linear regression to TRNSYS training data shown in Fig. 5a. The training data assumed internal latent gains (e.g. a latent gain per person is approximately 0.07 kg/h) and latent loads due to ventilation/infiltration. Another set of TRNSYS data shown in Fig. 5b was used as the validation data set. The inverse model showed satisfactory agreement with TRNSYS data for this type of analysis, with relative RMS error of 0.038.

2.2. Energy consumption

2.2.1. Cooling power

Heat pumps are components that consume the largest amount of cooling system energy, with the heat pump coefficient of performance (COP) representing the ratio between a cooling rate and consumed power. Although the COP is a function of a part-load ratio, evaporator air/water inlet conditions and condenser water/air inlet conditions, in the literature it is common to find HVAC system analyses that use a constant COP. This simplification might be acceptable, for example, when comparing the energy consumption of buildings with different facades or shading options. However, when using MPC to minimize the energy consumption, a constant COP would not give the optimal solution since it would not capture dependence of the performance on temperatures and part-load ratios. To characterize the heat pump performance, one could use manufacturer's performance curves for a specific heat pump. However, manufacturer's data are very limited, usually specified as an energy efficiency ratio (EER) evaluated at a single operating condition, or a seasonal energy efficiency ratio (SEER) evaluated for a single indoor temperature and some range of outside temperatures. For many advanced systems that can operate at wide range of conditions and loads, these data are not sufficient. Also, it is shown in Zakula et al. [36] that modest over-sizing of a variable-speed heat pump can be desirable, which suggests that even conventional systems could benefit from detailed heat pump performance data.

To characterize the performance of a specific heat pump, the modeling environment presented here uses the results of the heat

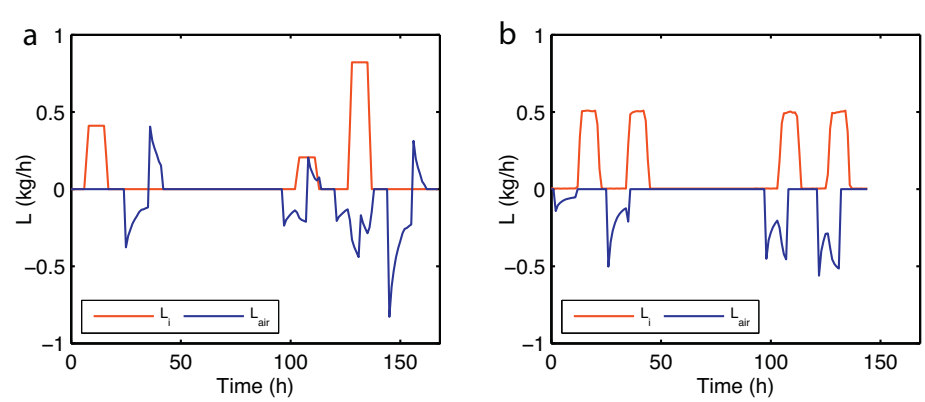

Fig. 5. Latent loads for (a) training data set and (b) validation data set.

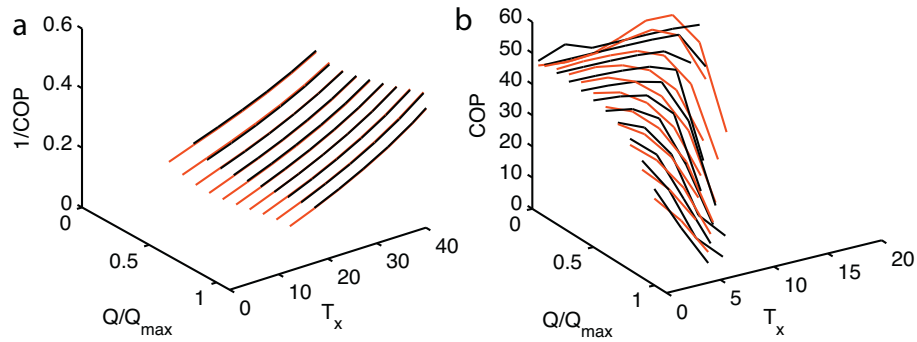

Fig. 6. (a) Third-order polynomial fit (red) to optimized specific power (black) in compressor-on mode and (b) fourth-order polynomial fit (red) to optimized COP (black) in economizer mode. Results are shown for water-to-air heat pump and water return temperature of 17 °C. (For interpretation of the references to color in this figure legend, the reader is referred to the web version of this article.)

pump static optimization. The result are obtained using a relatively detailed heat pump simulation model [37], and an optimization method presented in Zakula et al. [36]. To reduce computational time, the static optimization data are approximated with polynomial curves using the linear regression. Fig. 6a shows the results of the water-to-air heat pump static optimization (black) and fitted values (red) for a single water return temperature. A polynomial of the third order was fitted to specific power (1/COP) curves since it was found that the specific power data are easier to fit than the COP data. The fitted polynomial is a function of the part-load ratio (Q/Q_{max}), outside temperature, T_x and water return temperature $T_{w,return}$.

When the outside temperature is lower than the water supply temperature, the heat pump could run in the economizer mode, with the compressor turned off. However, in a case of smaller temperature differences across the evaporator and condenser (between air/water and refrigerant), the fan power will significantly increase. It is, therefore, incorrect to assume that the economizer mode will always give the lowest total power consumption. The advantage of the detailed heat pump model is its ability to optimize the economizer mode performance, and to enable the selection of the appropriate mode (normal versus economizer). Fig. 6b shows the results of the static optimization (black) for the same water-to-air heat pump, now running in the economizer mode. The results were fitted by a polynomial of the fourth order (red), but different than the normal mode, the COP values were now easier to fit than the specific power data. Having the detailed performance maps for both the normal and economizer mode enables the MPC optimization function to decide which mode consumes less power in cases when the outside temperature drops below the water supply temperature.

2.2.2. Transport power

When comparing the energy consumption between different HVAC systems (for example water and all-air systems), the difference in the transport power can be significant. Moreover, it was reported in Krarti and Henze [3] that excluding the transport power from the optimization can influence the optimization results and cost savings. Therefore, the MPC objective function should account for the transport power, especially when analyzing HVAC systems with a large transport power relative to the cooling/heating power. The fan/pump power P_{trans} is a function of a fan/pump characteristic, flow rates and total pressure losses throughout a building. The power at design conditions can be calculated using manufacturer's data, or alternatively, using the limitations given in ASHRAE Standard 90.1 [38]. Compared to supply fans, return fans have lower

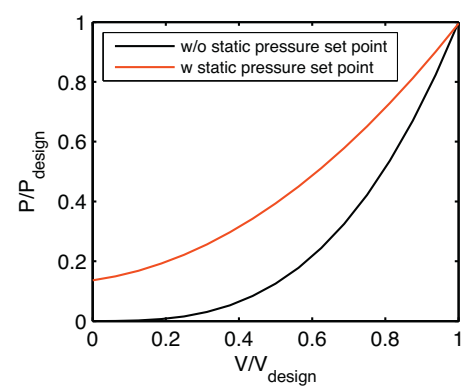

Fig. 7. Dimensionless fan power versus dimensionless air flow relation for VAV and ventilation system supply fan, with (red) and without (black) static pressure setpoint. (For interpretation of the references to color in this figure legend, the reader is referred to the web version of this article.)

power at design conditions due to lower pressure drops in return ducts.

An additional correlation is needed to calculate the power at flow rates different than designed. As explained in detail in Englander and Norford [39], the power for centrifugal devices varies as a cube of the flow only in cases where the pressure is solely a function of a flow. For these cases, the power goes to zero as the flow rate goes to zero, and can be described with the simple power law. For example, an exhaust fan is controlled based on the

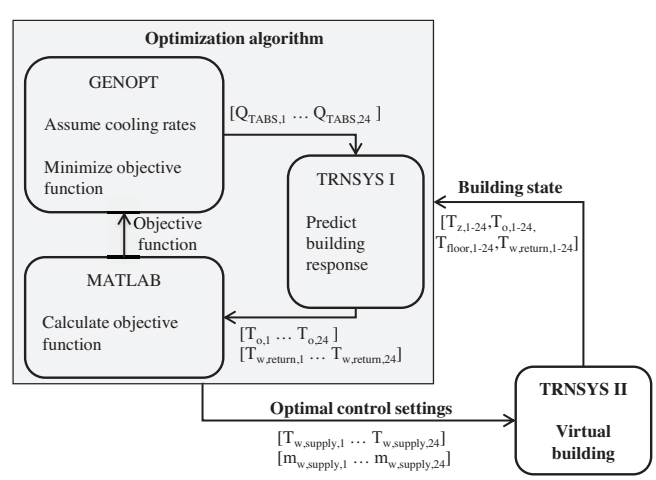

Fig. 8. MPC algorithm setup A.

airflow, and needs to overcome only losses in the exhaust duct. However, for devices that are pressure-regulated, and have a certain pressure to overcome, the fan power does not go to zero as the airflow goes to zero, but instead has a certain offset. Assuming a simple cube correlation and the zero power under no-flow conditions can significantly underestimate the power at low flow rates, as shown in Fig. 7. An example is a HVAC supply fan that has setpoint static pressure to overcome. Englander and Norford [39] developed a correlation (Eq. (12)) for the dimensionless fan power P/P_{design}, a function of the dimensionless pressure setpoint $p_{\text{set}}/p_{\text{design}}$, and the dimensionless airflow rate V/V_{design}. The correlation showed extremely good predictions when compared to experimental measurements for a VAV supply fan. While the modeling environment uses Eq. (12) to calculate the supply fan power, the return fans are modeled using the simple power law, where $Power = Constant(Airflow)^3$. The simplified approach is appropriate for return fans since they are usually controlled based on the flow rather than the pressure setpoint, having a zero power for no-flow conditions. The same power law is used to model the pump power for off-design conditions.

$$\frac{P}{P_{\text{design}}} = \left[1 - \left(\frac{1}{2}\frac{p_{\text{set}}}{p_{\text{design}}}\right)^{1.5}\right]\left[\left(1 - \frac{p_{\text{set}}}{p_{\text{design}}}\right)\left(\frac{V}{V_{\text{design}}}\right)^2 + \frac{p_{\text{set}}}{p_{\text{design}}}\right]\frac{V}{V_{\text{design}}} + \left(\frac{1}{2}\frac{p_{\text{set}}}{p_{\text{design}}}\right)^{1.5} \quad (12)$$

2.3. Optimization of the objective function

An example of objective function optimization is shown here for a case of minimizing the total cooling energy consumption, and with the planning horizon of 24 h. The objective function is a sum of the cooling power (P_{hp}), transport power required to deliver air/water to each zone (P_{trans}) and the temperature penalty related to thermal comfort (T_{penalty}). For each day the MATLAB function optimizes 24-h-ahead cooling rates using the objective function:

$$\text{OF} = \sum_{t=1}^{24}(P_{\text{hp}} + P_{\text{trans}} + T_{\text{penalty}}) \quad (13)$$

where

$$P_{\text{hp}} = Q_{\text{cc}}\text{COP}(Q/Q_{\text{max}}, T_{\text{fluid,e,in}}, T_{\text{fluid,c,in}}) \quad (14)$$

if $T_{\text{o}} < T_{\text{llim}}$

$$T_{\text{penalty}} = F_{\text{penalty}}(T_{\text{llim}} - T_{\text{o}})^2 \quad (15)$$

if $T_{\text{o}} > T_{\text{ulim}}$

$$T_{\text{penalty}} = F_{\text{penalty}}(T_{\text{o}} - T_{\text{ulim}})^2 \quad (16)$$

The function T_{penalty} penalizes values of the operative temperature that are outside the given limits. When choosing the appropriate penalty factor F_{penalty}, the amount of energy cost added to the penalty function (for the excursion just outside the comfort bounds) should be larger than the energy cost required to run the chiller to prevent that excursion [35]. For example, assume that the chiller uses 200 W at the lowest compressor speed and under the most conditions. In that case, F_{penalty} = 800 W/K^2 means that if the operative temperature drifts 0.5 K outside the comfort region, the cost of running the compressor will be lower than letting the temperature drift any further.

2.4. Optimization algorithm

Three different configurations were considered for the optimization algorithm, shown here as an example of optimizing the cooling system with TABS for the lowest electricity consumption. The optimization parameters were chiller cooling rates (Q_{TABS}) in each hour of the following 24 h.

Configuration A combines GenOpt [40] as the optimization engine with TRNSYS for the building's thermal and hygric response (Fig. 8). The objective function is calculated in MATLAB, but could also be calculated by developing a new module (type) in TRNSYS. GenOpt is a general optimization software that can be linked to other computer programs (including MATLAB, TRNSYS and EnergyPlus). Detailed instructions for the connection with TRNSYS can be found in Kummert [41]. The optimization method chosen from the GenOpt library is the combination of particle swarm optimization (PSO) and Hooke–Jeeves pattern search (HJPS). This method, as well as some other non-gradient optimization methods, are recommended in the software manual [40] for optimization problems that calculate the objective function using building modeling programs. PSO, inspired by a social behavior of, for example, bird flocking or fish schooling, has a swarm of particles moving around the search space, where the movements of individual particles are influenced by the improvements discovered by others in the swarm. This method is used in the first optimization stage to find an appropriate starting point for the HJPS method. HJPS, similar to the MATLAB built-in pattern search, takes steps in different search directions, modifying the step size and search direction every time a lower objective function cannot be found using the current step size.

In configuration B, the TRNSYS building model is replaced with the inverse model. The optimization algorithm combines GenOpt and MATLAB, where MATLAB is evaluating the objective function and building response (Fig. 9). The TRNSYS model is still used in the pre-optimization phase to create training data for the calculation of the inverse model coefficients.

Configuration C is using only MATLAB (Fig. 10), which reduces the model complexity and computational time. The optimization method is MATLAB's built-in pattern search algorithm, a non-gradient optimization method that does not guarantee finding the global minima (but neither do the gradient-based methods). However, as described in more detail in Wetter [40], gradient-based methods are not particularly suitable for the problems where the objective function is determined using building models, and can therefore be very dependent on building model tolerances. Furthermore, the chances of finding the global minima with the pattern-search method can be improved by choosing an appropriately large initial step and/or starting with a different initial point.

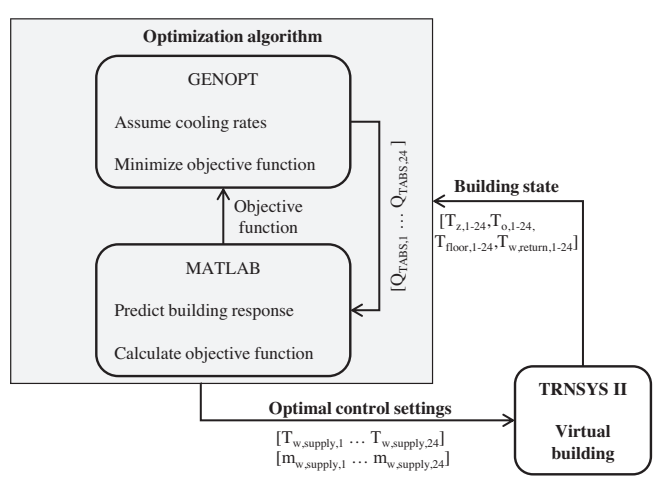

Fig. 9. MPC algorithm setup B.

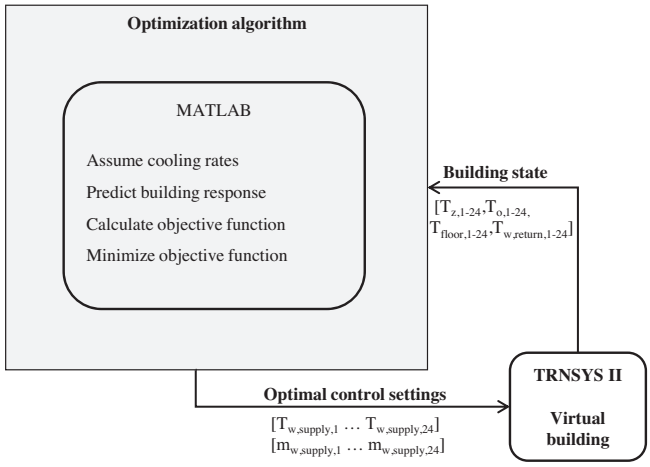

Fig. 10. MPC algorithm setup C.

After analyzing all thee configurations, configuration C was chosen for MPC analysis due to its simplicity and computational speed. Configuration A was abandoned due to its issues with initialization of variables and computational speed. This configuration was somewhat similar to the MPC models found in the literature, for which reported computational times were not suitable for fast simulation and implementation in real buildings. Moreover, connecting GenOpt, MATLAB and TRNSYS, or even GenOpt and TRNSYS would add to model complexity and possibly further degrade computational speed. Setting the GenOpt-MATLAB connection for configuration B was notably more challenging than setting the whole optimization in MATLAB (configuration C). Both configuration B and C predicted night precooling as the optimal strategy, with marginal differences in the energy consumption between the two configurations. However, while it took 30 s to optimize TABS cooling rates over 24 h with configuration C, the computational time with configuration B (with default GenOpt optimization settings) was approximately 45 min.

In the post-optimization phase, after finding the optimal cooling rates, the second TRNSYS model simulates the behavior of a virtual building using the optimal values as inputs. Although slower than the inverse model, the TRNSYS model predicts building response with better accuracy. The accurate predictions of model outputs (mainly temperature responses) are important for the next optimization steps since the inverse model requires the knowledge of the building's history.

The MPC schematic that optimizes VAV system cooling strategy would be very similar, with the VAV system cooling rate delivered to the room as the optimization parameter, and the airflow rates as inputs to the virtual building (the supply temperature for the VAV system is assumed to be constant).

3. Conclusion

The modeling environment (ME) presented here is developed to simulate buildings operated under MPC. The ME combines the optimization algorithm in MATLAB with two building models of different complexities, the building inverse model (based on transfer functions) and model from the commercially available building simulation program TRNSYS. Two additional modeling approaches are described, but were abandoned due to model complexity, issues with initialization of variables, and computational speed. The MATLAB optimization algorithm uses the pattern-search optimization method to find the optimal control strategy based on a predicted weather and internal gain forecast. The planning and execution horizon can be set depending on the accuracy of weather and load predictions. For example, in simulations were one has perfect predictions, both the planning and execution horizon are usually set to 24 h. In a real building, the execution horizon would be shortened to account for unexpected changes in weather forecast, internal loads and building responses.

To predict the building's thermal and hygric response on the proposed strategy, the optimization algorithm uses the inverse model based on transfer functions. The temperature/humidity is calculated as the sum of previous temperatures/humidities, and current and previous loads (e.g. cooling/heating rates, internal gains, latent gains). The number of past terms increases with the heaviness of the building structure. The inverse model coefficients are calculated using training data from TRNSYS or from a real building. It was demonstrated that, compared to the TRNSYS model, the inverse model can give very good predictions in significantly shorter time. After the optimization, the optimal values are sent to the virtual building modeled in TRNSYS. Although slower than the inverse model, the TRNSYS model allows the prediction of the building's response to the optimal control strategy with better accuracy. Having accurate predictions in the post-optimization phase is important since the TRNSYS model outputs (thermal and hygric history) are used by the inverse model in the next optimization step. In a real building, the TRNSYS model would be replaced with the response from the building automation system (BAS).

The example of the ME setup was shown for the cooling system with thermally activated building surfaces (TABS) and variable-air-volume (VAV) system operated under MPC, and with the objective of optimizing the daily electricity consumption. The objective function was the sum of the heat pump power required for air/water cooling, transport power and temperature penalty, where the temperature penalty ensured that the controlled variable (operative temperature) is inside the desired comfort range. The heat pump performance was optimized using the heat pump model developed from first principles. The static optimization was decoupled from the building optimization, and the optimized data were used in the ME by fitting the polynomials to the heat pump optimization results. The heat pump performance was also optimized for the economizer mode when the outside temperature was lower than the water temperature. Alternatively, one could use manufacturer's heat pump maps for a specific heat pump.

Although MPC is an emerging technology in the building industry, its implementation and analysis is greatly inhibited due to the lack of commercially or publicly available software tools. The ME presented here is open to the public, and can be provided upon request. It allows for the systematic study of primary factors influencing the dynamic control and savings potential for an individual building. Complex connections between building energy softwares and optimization algorithms are avoided by employing the simplified building model for the optimization. Except with TRNSYS, the ME can be used with other building softwares as well, as long as they account for building dynamics (e.g. EnergyPlus). Furthermore, the use of the simplified building model resulted in considerably shorter computational times then those found in the literature. For example, it took 30–60 s to optimize 24 cooling rates for a single-zone for a typical summer day (on the Windows 7 platform operated on Intel i5, 2.3 GHz dual-core processor). Computational time is especially relevant for the implementation in real buildings, for which the optimization needs to be performed each hour (or shorter) due to weather and load uncertainties. Finally, the ME is highly modular, enabling simulation and optimization of different HVAC systems and optimization objectives. The use of the ME for MPC analyses was demonstrated in the accompanying paper [42] for a VAV system, VRF system and parallel TABS and DOAS system. However, it can be expanded to other systems, such as chilled beams, fan-coils, active thermal storage, ground source heat exchanges, etc. The ME can also be employed to determine the cost

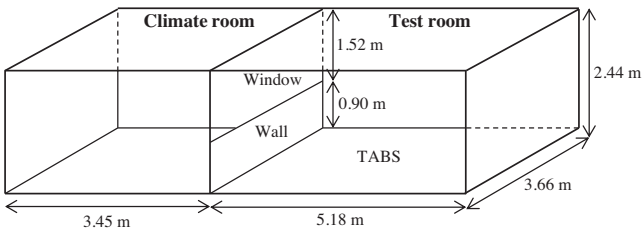

Figure A.1. Experimental room setup.

Table A.1
Experimental room construction

	Construction layers (inside to outside)
A. Wall	0.016 m gypsum board 0.089 m air gap and 0.05 × 0.1 m stud wall 0.11 m polyisocyanurate foam R-30 0.016 m gypsum board
B. Ceiling	0.016 m gypsum board 0.140 m air gap and 0.05 × 0.15 m joists 0.11 m polyisocyanurate foam R-30 0.013 m plywood
C. Window	Three 1.12 × 1.17 m double pain windows separated by 0.09 m frames
D. Floor	Vinyl tile floor 0.025 m plywood 0.09 m floor joists with 0.076 m polyisocyanurate foam R-20 Existing concrete floor
E. TABS	Three layers of 0.044 m concrete pavers 0.00076 m aluminum 0.04 m plywood subfloor with 0.013 m PEX pipes (0.3 m center-to-center spacing) D. Floor

penalty associated with the use of near-optimal control, or in parallel systems to determine the right split between each system, e.g. between TABS and air-system heating/cooling. In the ongoing work, the ME is used to optimize the cooling system for a building that participates in the energy market by providing the ancillary services.

Acknowledgments

The authors wish to acknowledge the MIT Energy Initiative, the Masdar Institute of Science and Technology, the National Science Foundation (EFRI-SEED award 1038230) and the Martin Family Society for their support of this research. They also thank Pacific Northwest National Laboratory for sharing the results of its study of low-lift cooling technology.

Appendix A. Experimental room description

See Fig. A.1 and Table A.1.

References

[1] J.E. Braun, Reducing energy costs and peak electrical demand through optimal control of building thermal storage, ASHRAE Transactions 96 (2) (1990) 876–888.
[2] K. Lee, J.E. Braun, Development and application of an inverse building model for demand response in small commercial buildings, in: Proceedings of SimBuild, 2004, pp. 1–12.
[3] M. Krarti, G.P. Henze, Real-time Predictive Optimal Control of Active and Passive Building Thermal Storage Inventory. Tech. Rep., State Technology Advancement Collaborative, 2005.
[4] P.R. Armstrong, W. Jiang, D. Winiarski, S. Katipamula, L.K. Norford, Efficient low-lift cooling with radiant distribution, thermal storage, and variable-speed chiller controls – Part 2: Annual use and energy savings, HVAC&R Research 15 (2) (2009) 402–432.
[5] S. Prívara, J. Široký, L. Ferkl, J. Cigler, Model predictive control of a building heating system: the first experience, Energy and Buildings 43 (2–3) (2011) 564–572.
[6] F. Oldewurtel, A. Parisio, C. Jones, D. Gyalistras, M. Gwerder, V. Stauch, B. Lehmann, M. Morari, Use of model predictive control and weather forecasts for energy efficient building climate control, Energy and Buildings 45 (2012) 15–27.
[7] N.T. Gayeski, P.R. Armstrong, L.K. Norford, Predictive pre-cooling of thermo-active building systems with low-lift chillers, HVAC&R Research 18 (5) (2012) 858–873.
[8] J. Alvarez, J. Redondo, E. Camponogara, J. Normey-Rico, M. Berenguel, P. Ortigosa, Optimizing building comfort temperature regulation via model predictive control, Energy and Buildings 57 (2013) 361–372.
[9] M. Gruber, A. Trüschel, J.-O. Dalenbäck, Model-based controllers for indoor climate control in office buildings – complexity and performance evaluation, Energy and Buildings 68 (Part A) (2014) 213–222.
[10] S. Wang, X. Jin, Model-based optimal control of VAV air-conditioning system using genetic algorithm, Building and Environment 35 (August (6)) (2000) 471–487.
[11] P. Bacher, H. Madsen, Identifying suitable models for the heat dynamics of buildings, Energy and Buildings 43 (7) (2011) 1511–1522.
[12] R. Bălan, J. Cooper, K.-M. Chao, S. Stan, R. Donca, Parameter identification and model based predictive control of temperature inside a house, Energy and Buildings 43 (2–3) (2011) 748–758.
[13] G. Mustafaraj, J. Chen, G. Lowry, Development of room temperature and relative humidity linear parametric models for an open office using BMS data, Energy and Buildings 42 (3) (2010) 348–356.
[14] S. Goyal, P. Barooah, A method for model-reduction of non-linear thermal dynamics of multi-zone buildings, Energy and Buildings 47 (2012) 332–340.
[15] S. Prívara, Z. Váňa, E. Žáčeková, J. Cigler, Building modeling: selection of the most appropriate model for predictive control, Energy and Buildings 55 (2012) 341–350.
[16] S. Wu, J.-Q. Sun, A physics-based linear parametric model of room temperature in office buildings, Building and Environment 50 (2012) 1–9.
[17] S. Prívara, J. Cigler, Z. Váňa, F. Oldewurtel, C. Sagerschnig, E. Žáčeková, Building modeling as a crucial part for building predictive control, Energy and Buildings 56 (2013) 8–22.
[18] P.V. Overschee, B.D. Moor, Subspace Identification for Linear Systems: Theory – Implementation – Applications, Kluwer Academic Publishers, Nowell, MA, 1999.
[19] M. Krarti, M.J. Brandemuehl, G.P. Henze, Evaluation of Optimal Control for Ice Storage Systems. Final Project Report for ASHRAE 809-RP, 1995.
[20] G.P. Henze, R.H. Dodier, M. Krarti, Development of a predictive optimal controller for thermal energy storage systems, HVAC&R Research 3 (3) (1997) 233–264.
[21] P.-D. Moroşan, R. Bourdais, D. Dumur, J. Buisson, Building temperature regulation using a distributed model predictive control, Energy and Buildings 42 (9) (2010) 1445–1452.
[22] G.P. Henze, Personal communication in April 2012.
[23] H.C. Spindler, L.K. Norford, Naturally ventilated and mixed-mode buildings – Part 2: Optimal control, Building and Environment 44 (4) (2009) 750–761.
[24] P. May-Ostendorp, G.P. Henze, C.D. Corbin, B. Rajagopalan, C. Felsmann, Model-predictive control of mixed-mode buildings with rule extraction, Building and Environment 46 (2) (2011) 428–437.
[25] C.D. Corbin, G.P. Henze, P. May-Ostendorp, A model predictive control optimization environment for real-time commercial building application, Journal of Building Performance Simulation 6 (3) (2013) 159–174.
[26] B. Coffey, F. Haghighat, E. Morofsky, E. Kutrowski, A software framework for model predictive control with GenOpt, Energy and Buildings 42 (7) (2010) 1084–1092.
[27] M. Wetter, P. Haves, A modular building controls virtual test bed for the integration of heterogeneous systems, in: Third National Conference of IBPSA-USA, Berkeley/California, 2008 https://gaia.lbl.gov/bcvtb
[28] G.P. Henze, A.R. Florita, M.J. Brandemuehl, C. Felsmann, H. Cheng, Advances in near-optimal control of passive building thermal storage, Journal of Solar Energy Engineering 132 (2) (2010) 271–280.
[29] A. Kerestecioglu, M. Swami, A. Kamel, Theoretical and computational investigation of simultaneous heat and moisture transfer in buildings: "effective penetration depth" theory, ASHRAE Transactions 96 (1) (1990) 447–454.
[30] C. Rode, M. Woloszyn, Whole-building Hygrothermal Modeling in IEA Annex 41. Thermal Performance of Exterior Envelopes of Whole Buildings, ASHRAE, Atlanta, 2007, pp. 1–15.
[31] D. Crawley, L. Lawrie, C. Pedersen, R. Liesen, D. Fisher, R. Strand, R. Taylor, R. Winkelmann, W. Buhl, Y. Huang, A. Erdem, EnergyPlus, a new-generation building energy simulation program, in: Proceedings of Building Simulation '99. vol. 1, 1999, pp. 81–88.
[32] S.A. Klein, et al., TRNSYS 17: A Transient System Simulation Program, Solar Energy Laboratory, University of Wisconsin, Madison, WI, 2010.
[33] J.E. Seem, Modeling of Heat Transfer in Buildings (Ph.D. thesis), Wisconsin University, Madison, USA, 1987.
[34] P.R. Armstrong, S.B. Leeb, L.K. Norford, Control with building mass – Part 1: Thermal response model, ASHRAE Transactions 112 (1) (2006) 449.
[35] N.T. Gayeski, Predictive Pre-cooling Control for Low-lift Radiant Cooling Using Building Thermal Mass (Ph.D. thesis), Massachusetts Institute of Technology, 2010.

[36] T. Zakula, P. Armstrong, L. Norford, Optimal coordination of heat pump compressor and fan speeds and subcooling over a wide range of loads and conditions, HVAC&R Research 18 (6) (2012) 1153–1167.
[37] T. Zakula, N.T. Gayeski, P.R. Armstrong, L.K. Norford, Variable-speed heat pump model for a wide range of cooling conditions and loads, HVAC&R Research 17 (5) (2011) 670–691.
[38] ASHRAE, Standard 90.1-2004: Energy Standard for Buildings Except Low-rise Residential Buildings, 2004.
[39] S.L. Englander, L.K. Norford, Variable speed drives: improving energy consumption modeling and savings analysis techniques, in: Proceedings of American Council for an Energy-Efficient Economy, Washington, DC, 1992.
[40] M. Wetter, GenOpt Manual: Generic Optimization Program, Version 2.1.0., University of California (through Lawrence Berkeley National Laboratory), Berkeley, 2008.
[41] M. Kummert, Using GenOpt with Trnsys 16 and Type 56, ESRU University of Strathclyde, Glasgow, 2007.
[42] T. Zakula, L.K. Norford, P.R. Armstrong, Advanced cooling technology with thermally activated building surfaces and model predictive control, Energy and Buildings (2014), http://dx.doi.org/10.1016/j.enbuild.2014.10.054, submitted for publication.
[43] EERE, DOE energy efficiency and renewable energy: Building energy software tools directory. Accessed April 2013.